

PAPER • OPEN ACCESS

Effect of Impact Hydroforming Loads on the Formability of AA5A06 Sheet Metal

To cite this article: S H Zhang *et al* 2018 *IOP Conf. Ser.: Mater. Sci. Eng.* **418** 012114

View the [article online](#) for updates and enhancements.

You may also like

- [Description of stress-strain response and evaluation of the formability for Al-Cu-Mg alloy under the impact hydroforming](#)
Da-Yong Chen, Shi-Hong Zhang, Yong Xu et al.
- [Stress & strain character of tube hydroforming and its application in processing analysis](#)
Hongyang Li, Song Yu and Jianhui Li
- [Effect of Geometric Parameters on Formability and Strain Path During Tube Hydroforming Process](#)
A Omar, K R Harisankar, Asim Tewari et al.



ECS
The
Electrochemical
Society
Advancing solid state &
electrochemical science & technology

DISCOVER
how sustainability
intersects with
electrochemistry & solid
state science research

Effect of Impact Hydroforming Loads on the Formability of AA5A06 Sheet Metal

S H Zhang¹, Y Ma^{1,2}, Y Xu¹, A A El-Aty¹, D Y Chen¹, Y L Shang¹, A I Pokrovsky³

¹ Institute of Metal Research, Chinese Academy of Sciences, Shenyang 110016, China

² School of Materials Science and Engineering, Dalian University of Technology, Dalian 116024, China

³ Physical Technical Institute, National Academy of Sciences of Belarus, Minsk 220141, Belarus

shzhang@imr.ac.cn

Abstract. Recently, aluminium (Al) alloys are increasingly used in the automobile and aerospace industries because of their light weight and corrosion resistance properties. However, the applications of these materials are limited due to their poor formability especially at room temperature. Although hydroforming technology is one of the approaches used to improve the formability of Al alloys, it still cannot fulfil the requirements of designers and manufacturers to form high-quality complex shaped components. It has been found that high-speed forming is able to improve the formability of low plasticity metals at room temperature. Thus, impact hydroforming (IHF) technology is proposed by combining the advantages of high-speed forming and hydroforming, and it was used to address the issues of quasi-static hydroforming. Accordingly, the aim of this study is to investigate the effect of IHF on the formability of AA5A06 sheet metal. An IHF bulge experiment setup was developed by making use of a light gas gun which can accelerate the projectile up to 300m/s. The results show that the formability of the AA5A06 increased under most of the impact velocities, and the equi-biaxial strain before failure of the IHF is 50% higher than that of quasi-static hydroforming at strain rate of $2 \times 10^3 \text{ s}^{-1}$. It is concluded that the IHF technology is an appropriate method to improve the formability of Al alloys and form complex shape components.

1. Introduction

Hydroforming technology has attracted much attention as an advanced lightweight forming technology, due to its advantages in making complex shaped part from light weight alloys such as aluminum alloys [1, 2]. Aluminum alloys have become more and more attractive for structural applications, known to the aerospace and automotive industries because of their superior properties such as low density and good corrosion resistance [3, 4]. The formability of aluminum sheet using hydroforming technology is not sufficient to form a product with complicated configurations [5]. Warm hydroforming technology can be used to enhance the formability of the aluminum [6], but the temperature of the forming process is strictly limited due to the microstructure requirement of the part [7]. A few years ago, high speed forming technologies were introduced [8]. The advantages of these technologies over a few traditional forming techniques are their ability to improve formability and reduce springback [9]. Considering the high speed forming can promote the metal formability, and the hydroforming has good surface quality and little geometric characteristic filling ability by adopting the



flexible medium, after combining the advantages of the two forming technologies, in this paper, the authors propose a novel forming technology named impact hydroforming (IHF).

Indeed, there are already many researchers in the dynamic field investigate the dynamic responses of the sheet or plate subjected to the impulsive loading under water, such as the underwater explosion [10, 11] or fluid-structure interactions (FSI) [12, 13]. Most of the previous investigations focused on blast energy absorption characteristic of structures, and the material like sandwich plates with foam layer is widely used.

The hydraulic bulge formability of sheet at various strain rates is investigated by many researchers in the metal forming field. Broomheas [14] is the first one who used bulge test to investigate the influence of strain rate on the strain to fracture of sheet metals. As a result, forming limit curve (FLC) of low carbon steel was determined successfully at strain rates of up to 70 s^{-1} . They observed that increasing strain rate leads to lowering the forming limits. High strain rate bulge experiments on 6111-T4 sheets were performed by Grolleau [15] using Split Hopkinson Pressure Bar (SHPB). The maximum strain rate was 500 s^{-1} . They calculated the equivalent strain of aluminum 6111-T4 sheets by the strain signal but did not compare with experiments value. This method was further refined by Ramezani [16] by replacing the fluid to rubber to investigate the AA6005-T6 sheet. The experiments results demonstrated that the strain of sheet increased with the impact velocity increasing. The strain of 3003 alloy sheet under strain rate range of $200\text{-}850 \text{ s}^{-1}$ is investigated by Justusson [17] by a shock tube. The ductility and plasticity of 3003 Al-Mn alloy displays obvious improvement at high strain rates. Kim [18] modified a high-speed stretch testing by adding special jigs used for high speed condition. He found that the FLC obtained from rigid steel punch high-speed bulge experiment is lower than that obtained from the static biaxial stretch forming region because the shear fracture induces the decrease of ductility of CQ and DP590.

Unlike previous researches of the dynamic domain, this paper takes the impulsive loading under water as a forming technology, and more focused on the dynamic formability of sheet subjected to IHF. The current study involves high strain rate (HSR) hydraulic bulge test of the aluminum 5A06 sheet with different impact velocities. The biaxial strain was obtained and the results are compared with the results of the quasi-static (QS) bulge.

2. Experiment procedure

2.1. Material

The material used in this investigation was AA5A06-O (Al-Mg alloy) sheet. The chemical compositions and microstructure of AA5A06 before testing were depicted in Table 1 and Figure 1.

Table 1. Nominal chemical compositions of AA5A06 detected by OES.

Element	Mg	Mn	Fe	Si	Ti	Zn	Cu	Be
Percent	6.50	0.54	0.16	0.06	0.06	<0.05	<0.05	0.0005



Figure 1. Microstructure of 5A06-O.

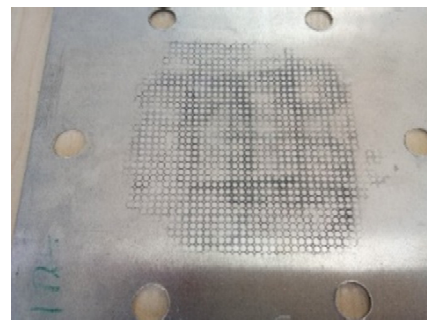


Figure 2. Specimen of HSR bulge test.

2.2. The bulge experiment under QS and HSR conditions

The diameter of the specimens used in this study were 160 mm for the QS bulge experiments. The specimens used in HSR were square blanks containing 6 holes with 12 mm diameter distributed at the 130mm diameter circle as shown in Figure 2. A series of 2.5 mm diameter circles were etched using an electrochemical method onto the sheet before testing, and these circles were used to calculate the strain. All along forming, the grids were deformed and their circular shapes changed into ellipses with the minor and major axes characterizing the direction of principal strains. The values of these principal strains at failure can be acquired through calculating the minor and major axes of the ellipses close to the fracture site and matching them with the initial diameter of the grids.

The setup used under QS condition was a conventional set-up for the bulge test as shown in Figure 3. The sheet was fixed between the binder and the lower die. The clamping force between the binder and lower die should be big enough to avoid sliding of the sheet between the dies by a hydraulic press. Through the test, the unclamped part of the specimen is forced to deform into the shape of hemisphere by constantly growing the pressure of the fluid which causes sheet deformation. The bulged sheet will fracture just after the deformation of the material exceeds its forming limit. There was a camera to record the deformation time to calculate the strain rate.

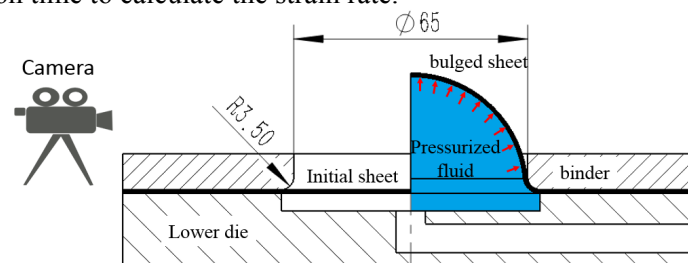


Figure 3. QS bulge test setup.

Figure 4 is the schematic of HSR testing system, the design concept is followed the principle of IHF. The projectile was fired out under the high pressure of the light gas gun, the projectile translated at high speed. The high-speed camera No. 1 recorded the moving process and this was used to calculate the velocity. Then the piston is impacted by the projectile. Then the projectile and piston impact the water together to produce high pressure impulse, the sheet will deform when the pressure impulse propagate to it. The process duration is very short, so the strain rate of the sheet was very high. The high-speed camera No. 2 was used to record the bulge duration, and fracture moment can be captured immediately when it happened. Different strain rates are able to be realized by setting the releasing pressure of light gas gun. The projectile consist of steel plate and plastic seat with a blind hole in it for avoiding the leak of gas during acceleration. Projectile weight 217g, piston weight 282g.

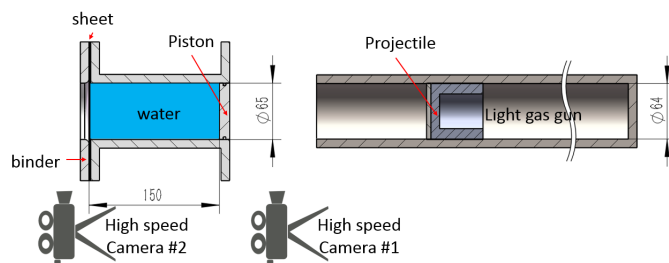


Figure 4. HSR bulge testing system.

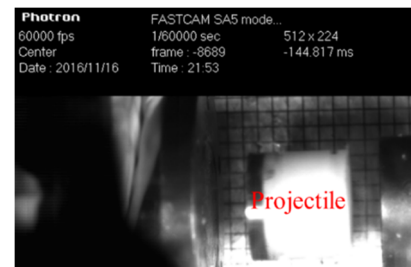


Figure 5. Projectile captured by high speed camera No. 1.

The experiments were repeated 3 times for each experimental condition. The QS experiments were taken by a hydraulic pump, and the HSR bulge tests were taken under 0.3MPa, 0.4MPa, 0.5MPa, 1MPa and 2MPa release pressure of the light gas gun. The calculation of the impact velocity of the projectile is assisted with the reference plate, the side length of the grid of the back reference plate is

10 mm, the capturing speed of high speed camera (No. 1) was set to 60000 fps, Figure 5 is one of the captured images, the number of the images was counted for going through 10 grids then the speed can be calculated out.

The impact velocities of projectile are listed in Table 2.

Table 2. Impact velocities of projectile.

Pressure (MPa)	0.3	0.4	0.5	1	2
Impact velocity (m/s)	103.92	121.48	134.16	189.74	268.33

The equal biaxial crack strain was measured as close as possible to the apex by the commercial sheet metal forming testing machine BCS-50BR. Due to off-line measurement, only the strain near to the crack can be detected, so the strain deviates a little from the absolute equal biaxial path.

Two etched circles i and j on the same specimen were measured after deformation, both of the major and minor strains of circle i should be larger than the corresponding strains of circle j , and the strain of the circle i should be closer to the equal biaxial line than circle j which is described as Equation (1), then repeat this process until the maximum circle was found for the same specimen. Afterwards, the same procedure will be implemented to all of other specimens.

$$\begin{cases} \varepsilon_1^i > \varepsilon_1^j, \varepsilon_2^i > \varepsilon_2^j \\ |\varepsilon_1^i - \varepsilon_2^i| < |\varepsilon_1^j - \varepsilon_2^j| \end{cases} \quad (1)$$

There are 4 indices used to compare the formability of HSR bulge tests with that of QS bulge tests: Effective fracture strain ($\bar{\varepsilon}$) of a circle was calculated according to Equation (2).

$$\bar{\varepsilon} = \frac{1}{3} \sqrt{2[(\varepsilon_1 - \varepsilon_2)^2 + (\varepsilon_2 - \varepsilon_3)^2 + (\varepsilon_3 - \varepsilon_1)^2]} \quad (2)$$

The increase of the effective strain ($\Delta\bar{\varepsilon}\%$) of HSR bulge tests compared with the QS bulge tests was defined by Equation (3).

$$\Delta\bar{\varepsilon}\% = \frac{\bar{\varepsilon}_{\text{HSR}} - \bar{\varepsilon}_{\text{QS}}}{\bar{\varepsilon}_{\text{QS}}} \% \quad (3)$$

The forming time (t) of the quasi-static bulge is about 60 seconds. The forming time (t) of the high strain rate test is calculated according to the number of images captured by the fast speed camera No. 2 and the time interval of 2 images. The capturing speed was set to 100,000 fps, which is 10 μs per image.

For the purposes of this investigation, the effective strain rate ($\dot{\bar{\varepsilon}}$) was the ratio of the effective strain and the forming time according to the definition as expressed in Equation (4).

$$\dot{\bar{\varepsilon}} = \frac{\bar{\varepsilon}}{t} \quad (4)$$

3. Results and discussion

All the specimens cracked except the 0.3MPa specimens of HSR bulge tests. The experimental specimens are shown in Figure 6, for each condition only one typical specimen was selected.

The major and minor strain of the biaxial position of the specimens after crack were plotted on Figure 7. Only one data point was selected for each specimen according to Equation (1). The data points position of 268.33 m/s is similar to that of the QS condition. The specimens of 103.92 m/s impact velocity are not cracked, hence data points are positioned lowest, this demonstrated that there is a limit velocity required for cracking the specimen. The data points of other impact velocities placed higher than that of QS condition, and 121.48 m/s is the optimal impact velocity to get maximum biaxial strain. The existing of optimal impact velocity is related to the crack mode. The low impact velocity deformation mode is the same to that of QS condition. The specimens will crack to several petals at higher impact velocity. The higher of the impact velocity, the more of the number of the crack petals, the deformation will be more evenly distributed at higher impact velocities. Therefore

there will be one critical impact velocity between the low impact velocity and the high impact velocity to get maximum strain.



Figure 6. Specimens after QS and HSR bulge tests (unit of impact velocity: m/s).

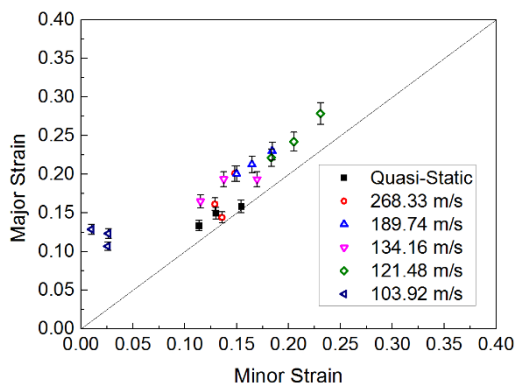


Figure 7. Equi-biaxial strain of the specimens of HSR and QS bulge experiments.

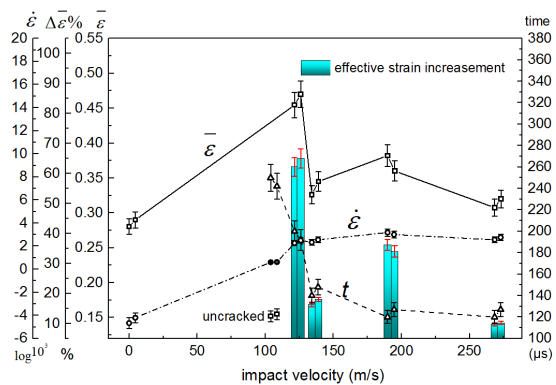


Figure 8. The 4 indices of the bulge experiment.

The four indices mentioned in 2.2 were plotted on Figure 8. The impact velocity of QS condition was seemed as 0. The data comes from two sets of experiments. The error of major or minor strain of etched circle is 5% according to the measurement equipment accuracy. Therefore the errors of $\bar{\epsilon}$ and $\Delta\bar{\epsilon}\%$ are the same to the error of major and minor strain. The error of forming time of HSR condition is 6% according to the capturing speed of the high speed camera No. 1. The maximum error of $\dot{\bar{\epsilon}}$ is 11% based on the errors of strain and time.

Overall, the effective strain declined with velocity increasing for the cracked specimens of HSR bulge. So there exists the optimal impact velocity for the impact hydroforming. The maximum increase of the effective strain of the optimal impact velocity compared with that of QS bulge is 62.18%. This proves that the impact hydroforming can increase the formability of aluminum sheet at room temperature. The trend of forming time is the same with the trend of effective strain, and it is from 100 to 250 μs . The effective strain rate of the QS bulge test is $4.67 \times 10^{-3} \text{ s}^{-1}$, the effective strain rate of non-crack HSR bulge is 608 s^{-1} , and the effective strain rate of other impact velocities are ranged $2.33\text{-}3.18 \times 10^3 \text{ s}^{-1}$. And the variation of the strain rate is very limited under the HSR crack ones.

4. Conclusions

The investigation of the present study demonstrated that the impact hydroforming is able to enhance the aluminum sheet formability at room temperature.

The improvement of the effective strain under HSR condition compared with that of QS condition is not monotonically increased with the impact velocity increasing due to the crack mode, there exists an optimal impact velocity. The maximum increase of the effective strain was 62.18% of the

specimens under the impact velocity of 121.48 m/s compared with the QS bulge ones. The effective strain rate of HSR bulge are ranged $2.33\text{-}3.18 \times 10^3 \text{ s}^{-1}$.

Acknowledgments

The authors gratefully acknowledge the External Cooperation Program of BIC, Chinese Academy of Sciences (174321KYSB20150020), Research Project of State Key Laboratory of Mechanical System and Vibration (MSV201708) and the Shenyang Science and Technology Planned Program (17-32-6-00). The authors also acknowledge the work of Homberg W, Djakow E and Akst O about pneumo-mechanical forming (ICHSF 2012).

References

- [1] Zhang S H 1999 Developments in hydroforming *J. Mater. Process. Technol.* **91** 236-44
- [2] Dohmann F and Hartl C 1996 Hydroforming-a method to manufacture light-weight parts *J. Mater. Process. Technol.* **60** 669-76
- [3] Nakai M and Eto T 2000 New aspect of development of high strength aluminum alloys for aerospace applications *Mater. Sci. Eng. A.* **285** 62-8
- [4] Miller W S, Zhuang L, Bottema J, Wittebrood A, De Smet P and Haszler A 2000 Recent development in aluminium alloys for the automotive industry *Mater. Sci. Eng. A.* **280** 37-49
- [5] Novotny S and Geiger M 2003 Process design for hydroforming of lightweight metal sheets at elevated temperatures *J. Mater. Process. Technol.* **138** 594-9
- [6] Palumbo G, Piccininni A, Guglielmi P and Di Michele G 2015 Warm HydroForming of the heat treatable aluminium alloy AC170PX *J. Manuf. Processes.* **20** 24-32
- [7] Mahabunphachai S and Koç M 2010 Investigations on forming of aluminum 5052 and 6061 sheet alloys at warm temperatures *Mater. Des.* **31** 2422-34
- [8] Gayakwad D, Dargar M K, Sharma P K and Rana R S 2014 A review on electromagnetic forming process *Procedia Mater. Sci.* **6** 520-7
- [9] Gerdooei M and Dariani B M 2008 Strain-rate-dependent forming limit diagrams for sheet metals *Proc. Inst. Mech. Eng. B: J. Eng. Manuf.* **222** 1651-9
- [10] Rajendran R and Narasimhan K 2006 Deformation and fracture behaviour of plate specimens subjected to underwater explosion-a review *Int. J. Impact Eng.* **32** 1945-63
- [11] Deshpande V S, Heaver A and Fleck N A 2006 An underwater shock simulator *Proc. Roy. Soc. Lond. A: Mat.* **462** 1021-41
- [12] Espinosa H D, Lee S and Moldovan N 2006 A novel fluid structure interaction experiment to investigate deformation of structural elements subjected to impulsive loading *Exp. Mech.* **46** 805-24
- [13] Wei X, Latourte F, Feinberg Z, Olson G and Espinosa H 2012 Design and identification of high performance steel alloys for structures, subjected to underwater impulsive loading *Int. J. Solids Struct.* **49** 1573-87
- [14] Broomhead P and Grieve R J 1982 The effect of strain rate on the strain to fracture of a sheet steel under biaxial tensile stress conditions *J. Eng. Mater. Technol.* **104** 102-6
- [15] Grolleau V, Gary G and Mohr D 2008 Biaxial testing of sheet materials at high strain rates using viscoelastic bars *Exp. Mech.* **48** 293-306
- [16] Ramezani M and Ripin Z M 2010 Combined experimental and numerical analysis of bulge test at high strain rates using split Hopkinson pressure bar apparatus *J. Mater. Process. Technol.* **210** 1061-9
- [17] Justusson B, Pankow M, Heinrich C, Rudolph M and Waas A M 2013 Use of a shock tube to determine the bi-axial yield of an aluminum alloy under high rates *Int. J. Impact Eng.* **58** 55-65
- [18] Kim S B, Huh H, Bok H H and Moon M B 2011 Forming limit diagram of auto-body steel sheets for high-speed sheet metal forming *J. Mater. Process. Technol.* **211** 851-62